Electronic Supplementary Material (ESI) for New Journal of Chemistry.

Insight on the Li_2S electrochemical process in a composite configuration electrode

Lorenzo Carbone[1†], Roberta Verrelli[1†], Mallory Gobet[2], Jing Peng[2,3], Matthew Devany[4], Bruno Scrosati[5], Steve Greenbaum[2,*] and Jusef Hassoun[1,6*]

[1] Sapienza University of Rome, Chemistry Department, Piazzale Aldo Moro, 5, 00185, Rome, Italy

[2] Department of Physics & Astronomy, Hunter College of the City University of New York, New York, New York 10065, United States

[3] Ph.D. Program in Chemistry, City University of New York, New York, NY 10016 United States

[4] Department of Chemistry and Biochemistry, Hunter College of the City University of New York, New York, New York 10065, United States

[5] Electtrochimica ed Energia, Rome, Italy (Presently at the Helmholtz Institute, Ulm, Germany)

[6] Department of Chemical and Pharmaceutical Sciences, Chemistry, University of Ferrara, Via Fossato di Mortara, 17, 44121, Ferrara, Italy

[†]*Author equally contributed*

Corresponding authors: jusef.hassoun@unife.it; steve.greenbaum@hunter.cuny.edu

Supplementary Information

In this section, the electrochemical behavior of the Li_2S-C-$(PEO)_{20}LiCF_3SO_3$ composite cathode, hereafter referred to as Li_2S–C–PEO, is studied at room temperature (i.e. 25°C) in lithium half-cell employing 1 mol kg^{-1} $LiNO_3$, 1 mol kg^{-1} $LiCF_3SO_3$, DOL:DME (1:1 w/w) electrolyte solution. Furthermore, a comparative study of the galvanostatic cycling performances of Li_2S–C–PEO composite and bare, $(PEO)_{20}LiCF_3SO_3$-free Li_2S-C cathodes, hereafter referred to as Li_2S–C, is provided in order to highlight the effects of the proposed composite configuration on electrode mechanical stability and kinetics (e.g. Li^+ diffusivity and charge transfer) upon cycling. An electrochemical impedance spectroscopy (EIS) study of the Li_2S-C cathode during the first de-lithiation and lithiation processes is also provided. The study of the first galvanostatic cycle of the Li_2S–C–PEO composite cathode in lithium half-cell is completed by ex-situ SEM analysis, confirming the reversibility of the electrochemical process and the enhanced electrode mechanical stability due to the proposed composite electrode formulation. This preliminary study may be fruitful for the development of alternative cell configurations for advances Li_2S-based energy systems.

Further insights on the first de-lithiation and following lithiation process of the Li_2S–C–PEO composite cathode are given by ex-situ SEM measurements at various states of charge and discharge, shown in **Figures S1 (A)** and **(B)**. The evolution of the composite electrode morphology upon cycling is shown in the four panels of **Fig. S1 (B)**. Li_2S aggregates, characterized by a peculiar lamellar morphology, are clearly detectable within the pristine electrode (marked by 1 in Fig S1). Following the first de-lithiation process (marked by 2 in Fig S1), amorphous sulfur is formed and Li_2S phase cannot be detected in the composite electrode. Upon the following lithiation process (marked by 3 in Fig S1), Li_2S is again formed, as confirmed by the re-appearance of lamellar morphology aggregates well dispersed within carbon and binder in the electrode. A further charge (marked by 4 in Fig S1), leads to the disappearance of Li_2S and traces of residual decomposition products may be detectable at the electrode surface. These results further evidence the reversibility of the redox process upon cycling. However, following prolonged cycling the electrode surface may be covered by consistent

SEI layer avoiding proper interpretation of the images. Therefore, SEM images after prolonged cycling for the electrodes are considered not suitable for a proper analysis and, therefore, not reported.

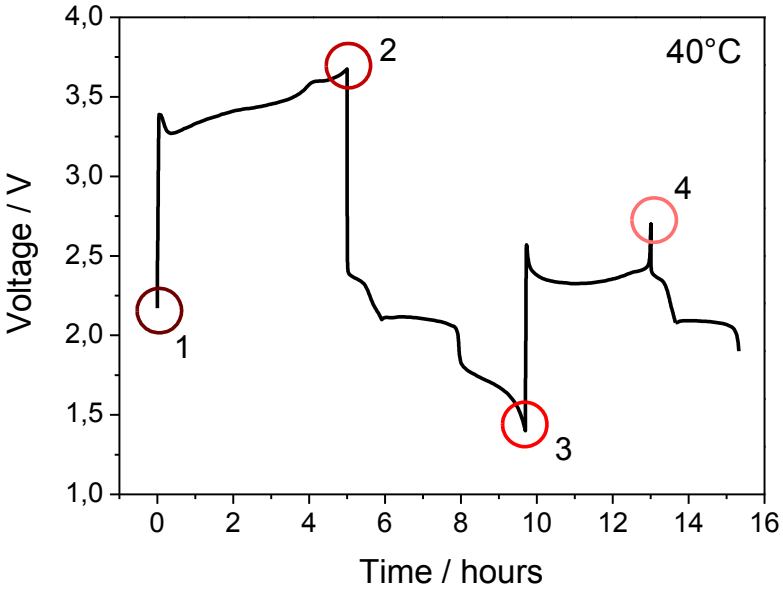

(A)

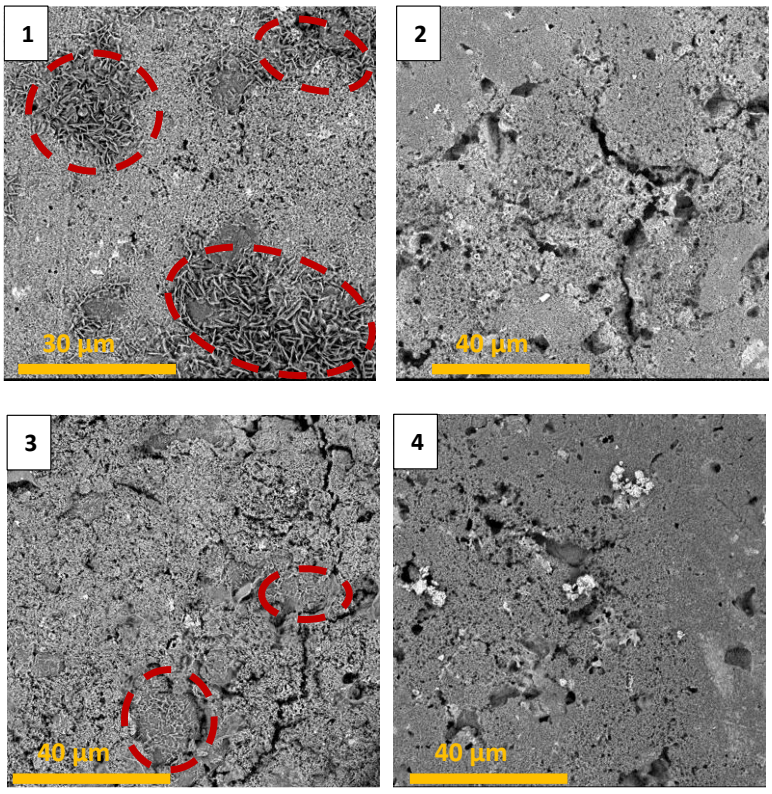

(B)

Figure S1

The room temperature galvanostatic cycling tests of the Li_2S–C–PEO cathode in lithium half-cell, using 1 mol kg^{-1} $LiNO_3$, 1 mol kg^{-1} $LiCF_3SO_3$, DOL:DME (1:1 w/w) electrolyte, at C/10 and C/5 rate are shown in **Figure S2 (A), (B)** and **(C), (D)**, respectively. When tested at lower C-rate (i.e. 116.6 mA g^{-1} with respect to Li_2S mass), the cell exhibits the characteristic multistep voltage signature of the Li_2S-based electrodes, with low polarization and voltage profiles stabilizing after the first activation cycle (Fig. S2A). During the first charge, the cell exhibits an activation barrier up to 3.5 V and then evolves through two main plateau regions centered at about 3.5 and 3.7 V that correspond to the progressive formation of short chain and long chain polysulfide species. Extra capacity is observed at voltages higher than 3.8 V, most reasonably due to parasitic reactions and to eventual contact losses between the Li_2S active material and the carbon electronic conductor. Upon lithiation, the described electrochemical processes are reversed at about 2.4 and 2.1 V, while the degradation of the $LiNO_3$ occurs, as expected, below 1.6 V. During the following charge-discharge cycles, stable voltage profiles centered between 2.2 and 2.4 V upon charge and between 2.4 and 2 V upon discharge indicate high reversibility of the overall electrochemical process and stability of the electrode upon cycling. Fig S2 **(B)** reveals that the cell delivers a specific capacity of about 1195 and 600 mAh g^{-1} during the first charge and discharge, respectively. The delivered specific capacity gradually shifts to a stable value of about 300 mAh g^{-1}, with Coulombic efficiency approaching 99% after the first few cycles. At increased cycling rate, i.e. at C/5, the various redox processes of the Li_2S–C–PEO electrode appear merged after the first charge and overlap in sloping trend with increased polarization (Fig. S2 **(C)**). The room temperature galvanostatic cycling test at C/5 shows a reversible specific capacity of about 120 mAh g^{-1} and Coulombic efficiency approaching 100% after the first few cycles (Fig. S2 **(D)**). A comparison of the cycling performances of the Li_2S–C–PEO cathode lithium half-cells at 40°C (Fig. 5 in the manuscript) and at room temperature is shown in Figure S2 **(E)** and **(F)**. Under the same current density (C/5), stable capacities of about 500 and 120 mAh g^{-1} are delivered by the Li_2S–C–PEO cathode in lithium half-cell at 40 and 25°C, respectively. As expected, the increase of the cell operating temperature translates into enhanced electrode kinetics in terms of both Li^+

diffusivity and charge transfer, in particular considering the high viscosity of the PEO binder. Furthermore, the effect of increased cell operating temperatures on the employed electrolyte viscosity and Li^+ transport properties have to be taken into account for explaining the observed electrochemical responses.

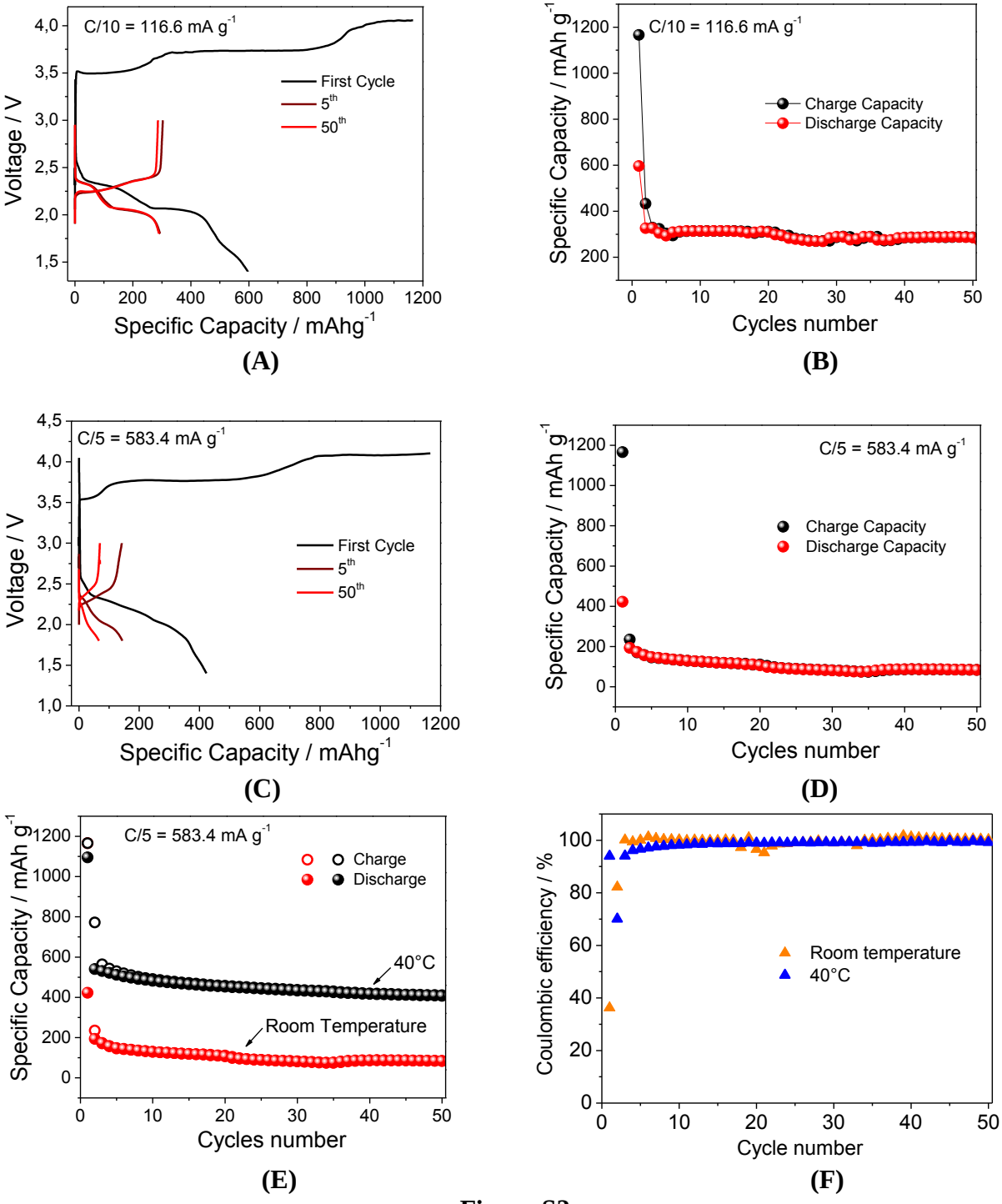

Figure S2

Figure S2 **(F)** shows comparable values of coulombic effiency both at 40°C and at room temperature. The first cycles inefficiency appears slightly lower at 40°C with respect to room temperature, while an efficiency approaching 99-100% is achievable at both the temperatures after stabilization of the charge-discharge cycles. The slight differences may be reasonably ascribed to additional polysulfide dissolution, limited to the first cycle, at higher temperature. These results suggest the temperature of 40°C as most suitable operating value for the proposed cell configuration.

Figure S3 shows the galvnostatic cycling response at C/10 C-rate and room temperature of the composite Li_2S–C–PEO and the bare Li_2S-C electrodes in lithium half-cell, employing $LiNO_3$–added, 1 mol kg^{-1} $LiCF_3SO_3$, DOL:DME (1:1 w/w) electrolyte. In particular, Figures S3 **(A)** and **(B)** display the voltage profiles of the composite Li_2S–C–PEO and bare Li_2S-C electrodes, respectively, while Figures S3 **(C)** and **(D)** show a comparison of the cycling performances of the two electrodes in terms of reversible specific capacity and coulombic efficiency, respectively. The voltage signatures in Fig. S3 (A) and (B) clearly indicate that polysulfide dissolution and consequent redox shuttle phenomena are consistently suppressed within the composite electrode configuration with respect to the bare Li_2S-C cathode. Indeed, the first charge voltage profile of the Li_2S-C cathode displays a very noisy trend after the first activation barrier, most reasonably ascribed to uncontrolled parasitic redox shuttle reaction or partial deterioration due to mechanical issues of the binder-free electrode. As expected, the following discharge cycle is very limited with respect to the one exhibited by the composite Li_2S–C–PEO electrode. The composite cathode exhibits two clearly detectable plateau regions centered at about 2.25 V and 2.35 V and at 2.3 and 2 V upon charge and discharge, respectively. Besides, after the first stabilization cycles, the voltage signature of the bare Li_2S-C electrode shows two plateau regions at 2.25 and 2.45 V upon charge while a sloping trend at about 2.4 V and a limited plateau at about 2 V are detectable upon discharge. Higher cell polarization is observed in the bare Li_2S-C electrode with respect to the composite one, thus suggesting that enhanced electrode kinetics and charge transfer are achieved by the exploitation $(PEO)_{20}LiCF_3SO_3$ binder. These results suggest that

the proposed composite electrode formulation is a viable strategy to suppress active material loss, polysulfide dissolution and redox shuttle phenomena upon cycling. The enhanced cycling performances of the composite electrode with respect to bare Li_2S-C indicate improved Li^+ diffusivity due to the conductive $(PEO)_{20}LiCF_3SO_3$ network between the active material and the conductive carbon. Figures S3 **(C)** and **(D)** compare the cycling performances at C/10 and room temperature of the composite Li_2S–C–PEO and bare, $(PEO)_{20}LiCF_3SO_3$-free electrode in terms of delivered capacity and Coulombic efficiency, respectively. The bare Li_2S-C electrode exhibits very limited reversible capacity of about 70 mAh g^{-1} while, within the same cycling conditions, the composite Li_2S–C–PEO cathode stably delivers a reversible capacity of about 300 mAh g^{-1} (i.e. a value more than three times higher than the one of bare Li_2S-C).

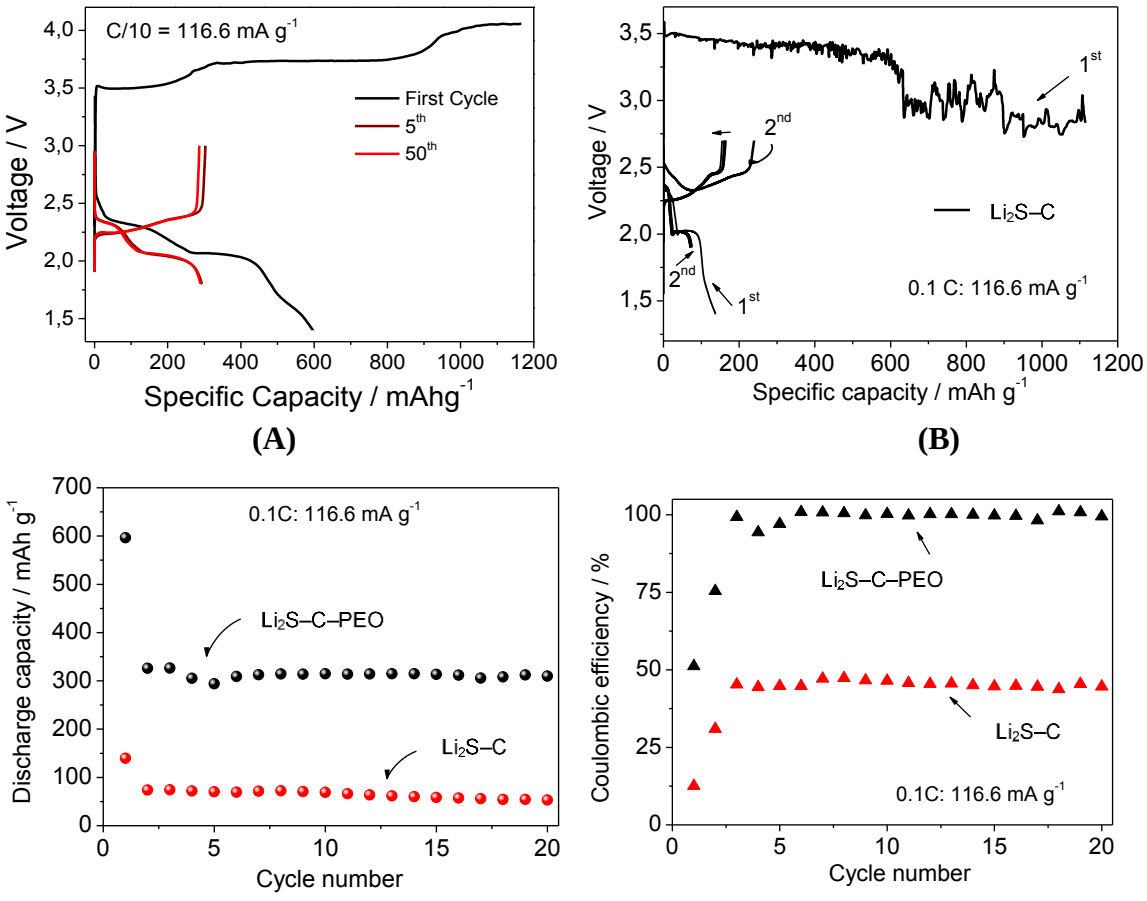

Figure S3

Figure S3 **(D)** evidences that the exploitation of a composite electrode configuration results in reduced active material losses and enhanced efficiency of the overall electrochemical process. Indeed, the columbic efficiency approaches 100% after the first few cycles for the composite Li_2S–C–PEO electrode and drops down to values lower than 50% for the $(PEO)_{20}LiCF_3SO_3$-free Li_2S-C electrode, thus suggesting uncontrolled polysulfide dissolution phenomena. Moreover, the obtained results suggest that the $(PEO)_{20}LiCF_3SO_3$ binder within the composite electrode configuration may reasonably enhance the electrode mechanical stability by avoiding active material segregation upon cycling and undesired contact losses and electrode pulverization.